Scientific Research Publishing

Journal of Power and Energy Engineering, 2025, 13(10), 144-169
https://www.scirp.org/journal/jpee
ISSN Online: 2327-5901
ISSN Print: 2327-588X

Intelligent Control of an SVC by Fuzzy Logic for Optimizing Dynamic Stability in a THT Network

Amos Omboua Eyandzi[1], Rodolphe Gomba[1], Nianga-Apila[1], Flory Lidinga Mobonda[2], Timothée Nzongo[3], Tite Lawd Ngouloubi[1], Rozan Etoua Ndouniama[4]

[1]Polytechnic Superior National School (ENSP), Marien Ngouabi University, Brazzaville, Congo
[2]Laboratory of Electrical Engineering, ISTA-Kinshasa, Democratic Republic of the Congo (DRC)
[3]Faculty of Sciences and Techniques, Marien Ngouabi University, Brazzaville, Congo
[4]Faculty of Letters, Arts and Human Sciences (FLASH), Marien Ngouabi University, Brazzaville, Congo
Email: ombouaweb@gmail.com

How to cite this paper: Omboua Eyandzi, A., Gomba, R., Nianga-Apila, Lidinga Mobonda, F., Nzongo, T., Ngouloubi, T.L. and Etoua Ndouniama, R. (2025) Intelligent Control of an SVC by Fuzzy Logic for Optimizing Dynamic Stability in a THT Network. *Journal of Power and Energy Engineering*, **13**, 144-169.
https://doi.org/10.4236/jpee.2025.1310010

Received: September 12, 2025
Accepted: October 27, 2025
Published: October 30, 2025

Abstract

Voltage stability is a major challenge for African industrial power networks, where highly inductive loads and variable consumption profiles compromise supply quality. This article presents the design and evaluation of a Static Var Compensator (SVC) controlled by a Mamdani fuzzy regulator, applied to the industrial network of Maloukou (220/110 kV) in Congo-Brazzaville. After recalling the analytical stability criteria and establishing the mathematical model of the SVC, the fuzzy regulator is developed and then integrated into a Simulink environment. Comparative simulations highlight a clear improvement over PI control: stabilization time reduced to less than 0.45 s, voltage maintained within the 0.98 - 1.02 p.u. range, damping of transient oscillations, and about 15% reduction in active losses. Beyond these performances, fuzzy logic proves robust against realistic disturbances (measurement noise, processing delays, sudden load variations), confirming its relevance as a tool for modernizing African power networks. This work paves the way for extensions towards hybrid regulators and the integration of intelligent solutions to support the energy transition in Central Africa.

Keywords

Voltage Stability, Static Var Compensator (SVC), Mamdani Fuzzy Logic, Industrial Power Networks, Reactive Compensation, FACTS, Congo-Brazzaville

1. Introduction

Voltage stability remains one of the major challenges of high- and extra-high-voltage power networks, particularly in developing countries where rapid industrialization is accompanied by highly variable loads and often undersized infrastructures. In Congo-Brazzaville, the industrial zone of Maloukou perfectly illustrates this issue: the growing demand and the integration of heavy loads with strongly inductive characteristics lead to voltage drops, persistent oscillations, and a deterioration of service quality. These phenomena compromise supply continuity and system reliability, and call for more effective regulation solutions than conventional approaches [1]-[6].

Among FACTS devices (*Flexible AC Transmission Systems*), the Static Var Compensator (SVC) is a reference technology for reactive power compensation and improvement of dynamic stability. However, its effectiveness directly depends on the adopted control strategy. Classical PI-type regulators, although simple and widely used, show their limits when facing nonlinear, uncertain, and rapidly varying operating conditions. They often lead to slow, oscillatory responses that are sensitive to external disturbances [7]-[10].

In this context, the integration of artificial intelligence techniques offers new perspectives. Fuzzy logic, in particular, has emerged as a robust and flexible control approach, capable of handling imprecise information and reproducing linguistic reasoning close to human expertise. It thus enables continuous adaptation of the regulation action to rapid variations in system state, where linear regulators fail. Several recent works have demonstrated the relevance of this approach for improving voltage stability and reducing losses in different power system contexts, but few studies have focused on African networks, which are nevertheless characterized by specific constraints of instrumentation and reliability [11]-[14].

The objective of this article is to design, model, and evaluate an SVC controlled by a Mamdani fuzzy regulator, applied to the industrial network of Maloukou. After recalling the stability criteria and mathematically modeling the system, the fuzzy regulator is developed and integrated into a Simulink environment. Comparative simulations highlight the superior performance of fuzzy control over PI, particularly in terms of stabilization time, loss reduction, and robustness to disturbances. This work stands out by its aim to adapt an advanced intelligent control technique to Congolese industrial realities and constitutes an original contribution to the modernization and reliability of power networks in Central Africa.

2. Methodology

The dynamic stability of extra-high-voltage (THT) power networks has been at the heart of electrical engineering research for several decades, particularly with the rise of intermittent energies and the increasing complexity of network architectures. Faced with these challenges, FACTS devices (Flexible AC Transmission Systems) have become essential tools to improve the dynamic performance of the system. Among them, the Static Var Compensator (SVC) occupies a central place

due to its ability to quickly adjust the reactive power injected or absorbed, thus contributing to the maintenance of a stable voltage [10] [15] [16].

Traditionally, SVCs are controlled using linear regulators, such as PID controllers, or through deterministic models based on simplifying assumptions. While these methods offer good efficiency under nominal conditions, their performance decreases as soon as the system is subjected to rapid variations, nonlinearities, or structural uncertainties. In addition, they often require manual recalibration and are poorly suited to the changing environments encountered today in modern power networks [17] [18].

In this perspective, numerous studies have explored advanced control strategies, such as adaptive control, robust control, and approaches based on artificial intelligence. Among these, fuzzy control has distinguished itself through its ability to handle uncertainty, to integrate heuristic rules derived from human expertise, and to produce smooth responses even in the absence of precise models. Several works have demonstrated its effectiveness in controlling complex electrical systems, particularly for voltage regulation and transient stability [19]-[21].

Hybrid approaches combining fuzzy logic with other techniques such as neural networks, evolutionary algorithms, or ANFIS (Adaptive Neuro-Fuzzy Inference System) have also emerged, with promising results. However, few studies have focused on a targeted and optimized application of fuzzy logic specifically applied to the control of an SVC in a disturbed THT network, while taking into account real-time performance constraints and robustness against load variations [21] [22].

It is in this context that the present research is positioned, aiming to fill this gap by proposing a dedicated fuzzy controller, optimized and tested in scenarios representative of real operating conditions of an THT network.

2.1. Small-Signal Dynamic Analysis

The power system with SVC is modelled by a set of differential-algebraic equations (DAE) [23] [24]:

$$\dot{x} = f\left(x, y, u, p\right), \tag{1}$$

$$0 = g\left(x, y, u, p\right), \tag{2}$$

where: The system is described by four sets of variables: the dynamic states $x \in \mathbb{R}^n$ (machines, AVR, filters, SVC controller), the algebraic variables $y \in \mathbb{R}^m$ (bus voltages, angles, currents, powers), the control inputs $u \in \mathbb{R}^r$ (regulator setpoints, voltage references), and finally the parameters p (impedances, time constants, limits).

2.1.1. Linearization

An equilibrium point $\left(x_0, y_0, u_0\right)$ satisfies $f\left(x_0, y_0, u_0, p\right) = 0$ and $g\left(x_0, y_0, u_0, p\right) = 0$. Defining deviations $\Delta x = x - x_0$, $\Delta y = y - y_0$, $\Delta u = u - u_0$ and linearizing (1)-(2) to first order, we obtain:

$$\Delta\dot{x} = f_x \Delta x + f_y \Delta y + f_u \Delta u, \tag{3}$$

$$0 = g_x \Delta x + g_y \Delta y + g_u \Delta u, \tag{4}$$

with $f_x = \left.\frac{\partial f}{\partial x}\right|_0$, $g_y = \left.\frac{\partial g}{\partial y}\right|_0$, etc. Under the standard assumption of non-singularity of g_y, (4) gives:

$$\Delta y = -g_y^{-1} g_x \Delta x - g_y^{-1} g_u \Delta u. \tag{5}$$

Injecting (5) into (3), we obtain a reduced state model:

$$\Delta \dot{x} = A\Delta x + B\Delta u, \text{ with } \boxed{A = f_x - f_y g_y^{-1} g_x, B = f_u - f_y g_y^{-1} g_u.} \tag{6}$$

The output of interest can be expressed in linearized form as $\Delta z = C\Delta x + D\Delta u$ if necessary. The SVC is inserted into the state model in two equivalent forms:

- **Algebraic**: imposed reactive injection

$$Q = -V^2 B_{\text{eq}}, \quad g(x, y, u, p) = 0 \tag{7}$$

with B_{eq} defined as a control variable.

- **Dynamic**: measurement-controller-command loop, where the internal states (filters, delays, saturations) are integrated into x and the setpoints into u.

In both cases, the controller (PI or fuzzy) acts on the global dynamics through the linearized structure of the system:

$$\dot{x} = Ax + Bu, \; A \mapsto A + f_y g_y^{-1} g_x, \; B \mapsto B + f_y g_y^{-1} g_u \tag{8}$$

which makes explicit the network-controller coupling.

2.1.2. Stability and Damping Criteria

The stability of the linearized system is governed by the spectrum of matrix A. The condition for asymptotic stability is written as:

$$\Re\{\lambda_i\} < 0, \; \forall i \tag{9}$$

with indicators such as the spectral abscissa $\alpha(A) = \max_i \Re\{\lambda_i\}$ (measure of the return speed), and the modal damping ratio, for a complex pair $\lambda = \sigma \pm j\omega$:

$$\zeta = -\frac{\sigma}{\sqrt{\sigma^2 + \omega^2}}, \; \zeta \geq \zeta_{\min} \; (\text{typically } 10\% \sim 15\%) \tag{10}$$

The evaluation of a regulator (PI or fuzzy) also relies on: (i) participation factors (dominant states), (ii) controllability/observability of critical modes, (iii) modal sensitivity to key parameters ($\mathrm{d}\lambda/\mathrm{d}k$).

The practical procedure includes: the computation of the equilibrium point by *load-flow*, the linearization and reduction of the DAE equations, the spectral analysis of A, then the iterative tuning of the regulator until the desired damping margins are satisfied. This linearized framework thus provides a quantitative and reproducible metric to compare SVC control strategies on the dynamic voltage stability.

2.2. Mathematical Modelling

2.2.1. Model of HT/THT Transmission Lines

Consider a differential line element of length $\mathrm{d}x$, characterized by the distributed parameters per unit length: resistance R [Ω/m], inductance L [H/m],

conductance G [S/m], and capacitance C [F/m]. In sinusoidal steady state (phasor representation at angular frequency ω), the application of Kirchhoffs laws gives:

$$V(x)-V(x+\mathrm{d}x)=(R+\mathrm{j}\omega L)I(x)\mathrm{d}x, \tag{11}$$

$$I(x+\mathrm{d}x)-I(x)=(G+\mathrm{j}\omega C)V(x)\mathrm{d}x. \tag{12}$$

Dividing by $\mathrm{d}x$ and letting $\mathrm{d}x\to 0$, we obtain the *telegraphers equations*:

$$\frac{\partial V}{\partial x}(x)=-(R+\mathrm{j}\omega L)I(x), \tag{13}$$

$$\frac{\partial I}{\partial x}(x)=-(G+\mathrm{j}\omega C)V(x). \tag{14}$$

Differentiating (13) with respect to x and substituting (14), we obtain the wave equations:

$$\frac{\partial^2 V}{\partial x^2}(x)=\gamma^2 V(x),\quad \frac{\partial^2 I}{\partial x^2}(x)=\gamma^2 I(x), \tag{15}$$

where

$$\begin{aligned}&\gamma=\sqrt{(R+\mathrm{j}\omega L)(G+\mathrm{j}\omega C)}\ \ (\text{propagation constant}),\\ &Z_c=\sqrt{\frac{R+\mathrm{j}\omega L}{G+\mathrm{j}\omega C}}\ \ (\text{characteristic impedance}).\end{aligned} \tag{16}$$

The general solutions of (15) are exponential waves. Setting $x=0$ at the receiving end and $x=l$ at the sending end:

$$V(x)=V^{+}\mathrm{e}^{-\gamma x}+V^{-}\mathrm{e}^{+\gamma x}, \tag{17}$$

$$I(x)=\frac{1}{Z_c}V^{+}\mathrm{e}^{-\gamma x}-\frac{1}{Z_c}V^{-}\mathrm{e}^{+\gamma x}. \tag{18}$$

By applying the boundary conditions (V_r, I_r) at the receiving end and (V_s, I_s) at the sending end, one obtains the *transmission relation*:

$$\begin{bmatrix}V_s\\ I_s\end{bmatrix}=\underbrace{\begin{bmatrix}\cosh(\gamma l) & Z_c\sinh(\gamma l)\\ \dfrac{1}{Z_c}\sinh(\gamma l) & \cosh(\gamma l)\end{bmatrix}}_{\equiv\begin{bmatrix}A & B\\ C & D\end{bmatrix}}\begin{bmatrix}V_r\\ I_r\end{bmatrix},$$
$$A=D=\cosh(\gamma l),\ B=Z_c\sinh(\gamma l),\ C=\frac{1}{Z_c}\sinh(\gamma l). \tag{19}$$

Useful limiting cases.

- **Short line** (small l, $G\simeq 0$): $\gamma l\ll 1$, $\cosh(\gamma l)\approx 1$, $\sinh(\gamma l)\approx \gamma l$, $Z_c\approx\sqrt{(R+\mathrm{j}\omega L)/(\mathrm{j}\omega C)}$.
- **Purely reactive line** ($R=G=0$): $\gamma=\mathrm{j}\beta$, $A=D=\cos(\beta l)$, $B=\mathrm{j}Z_c\sin(\beta l)$, $C=\mathrm{j}Z_c^{-1}\sin(\beta l)$.

We seek $S_R=P_R+\mathrm{j}Q_R=V_rI_r^{*}$. From (19),

$$I_r = \frac{V_s - AV_r}{B} \Rightarrow S_R = V_r I_r^* = V_r \frac{V_s^* - A^* V_r^*}{B^*} = \frac{V_r V_s^*}{B^*} - \frac{A^*}{B^*}|V_r|^2. \tag{20}$$

Thus,

$$P_R = \Re\left\{\frac{V_r V_s^*}{B^*} - \frac{A^*}{B^*}|V_r|^2\right\},\ Q_R = \Im\left\{\frac{V_r V_s^*}{B^*} - \frac{A^*}{B^*}|V_r|^2\right\}. \tag{21}$$

These expressions simplify easily in the particular cases above (e.g. $R = G = 0$).

2.2.2. Voltage Stability Criteria

The voltage stability of a transmission system can be studied using the two-bus Thvenin equivalent model, where a source $V_{\text{th}}\angle 0$ is connected to a load bus $V\angle\delta$ through the impedance $Z_{\text{th}} = R_{\text{th}} + jX_{\text{th}}$. The absorbed power is $S = P + jQ$. In the classical case of HT/THT lines where $R_{\text{th}} \ll X_{\text{th}}$, we approximate $Z_{\text{th}} \simeq jX$. The active and reactive powers at the load bus are then expressed as [24] [25]:

$$\boxed{P = \frac{VV_{\text{th}}}{X}\sin\delta,\ Q = \frac{V}{X}\left(V_{\text{th}}\cos\delta - V\right).} \tag{22}$$

By eliminating δ, we obtain the Q-V characteristic:

$$\boxed{Q(V;P) = \frac{1}{X}\left(V_{\text{th}}\sqrt{V^2 - k^2} - V^2\right),\ k = \frac{PX}{V_{\text{th}}}.} \tag{23}$$

The slope $\partial Q/\partial V$ defines the stability margin. The critical point, corresponding to the *nose* of the Q-V curve, is given by:

$$\boxed{V_{\text{crit}}^2 = \left(\frac{PX}{V_{\text{th}}}\right)^2 + \frac{V_{\text{th}}^2}{4}.} \tag{24}$$

For $V > V_{\text{crit}}$, the system operates in a stable zone where reactive power injection increases voltage ($\partial Q/\partial V < 0$). Conversely, as $V \to V_{\text{crit}}$, the margin vanishes and the system approaches voltage collapse.

2.2.3. Kessels *L* Index

We partition the bus admittance matrix Y_{bus} into load buses L and generator buses G [26]:

$$\begin{bmatrix} I_L \\ I_G \end{bmatrix} = \begin{bmatrix} Y_{LL} & Y_{LG} \\ Y_{GL} & Y_{GG} \end{bmatrix} \begin{bmatrix} V_L \\ V_G \end{bmatrix} \tag{25}$$

Isolating V_L,

$$V_L = -Y_{LL}^{-1}Y_{LG}V_G + Y_{LL}^{-1}I_L \triangleq FV_G + Z_{eq}I_L, \tag{26}$$

where $F \triangleq -Y_{LL}^{-1}Y_{LG}$ and $Z_{eq} \triangleq Y_{LL}^{-1}$. For each load bus $i \in L$, we define the supporting voltage. We can see $E_i \triangleq \sum_{k\in G} F_{ik}V_k$ as the Thvenin voltage seen at bus i if the injections I_L were zero. $E_i \triangleq \sum_{k\in G} F_{ik}V_k$. The Kessel index is then

$$\boxed{L_i \triangleq \left|1 - \frac{E_i}{V_i}\right| = \left|1 - \sum_{k\in G} F_{ik}\frac{V_k}{V_i}\right|,\ i \in L.} \tag{27}$$

When the network is far from collapse, $|E_i/V_i| \approx 1$ in magnitude and the argument is small $\Rightarrow L_i \simeq 0$. As the stability limit is approached, the supporting capacity of the G buses no longer compensates the local drop: the ratio E_i/V_i deviates from the vicinity of 1 and $L_i \to 1$. A global indicator is $L_{\max} \triangleq \max_{i \in L} L_i$; the closer $L_{\max}$ is to 1, the lower the voltage stability margin.

The power flow in polar coordinates is written as $F(\theta,V) = \left[P(\theta,V) \quad Q(\theta,V)\right]^{\top}$. The Newton Jacobian matrix is

$$J(\theta,V) = \begin{bmatrix} \dfrac{\partial P}{\partial \theta} & \dfrac{\partial P}{\partial V} \\ \dfrac{\partial Q}{\partial \theta} & \dfrac{\partial Q}{\partial V} \end{bmatrix} \tag{28}$$

By eliminating the angles through Schur reduction (assuming $\partial P/\partial\theta$ invertible at regular points), we obtain the reduced Jacobian in voltage

$$\boxed{J_R \triangleq \frac{\partial Q}{\partial V} - \frac{\partial Q}{\partial \theta}\left(\frac{\partial P}{\partial \theta}\right)^{-1}\frac{\partial P}{\partial V}.} \tag{29}$$

Loss of solvability (voltage collapse) is characterized by the singularity of J; equivalently, by the loss of positive definiteness/singularity of J_R. Numerically, the smallest singular value of J (or J_R) decreases towards 0 as the critical point is approached [23] [24].

2.2.4. Local Closed-Loop Analysis with the Fuzzy Regulator

Around the operating point (x_0, y_0, u_0), the plant admits the reduced linear model $\Delta\dot{x} = A\Delta x + B\Delta u$, with the regulated voltage $\Delta V = C_v \Delta x$ (for a suitable row selector C_v). The Mamdani fuzzy law $u = \mathcal{F}(e, \Delta e)$, with $e = V_{\text{ref}} - V$, is Frchet differentiable at $(e, \Delta e) = (0,0)$; its tangent plane defines the local gains

$$K_e \triangleq \left.\frac{\partial \mathcal{F}}{\partial e}\right|_0, \quad K_{\dot{e}} \triangleq \left.\frac{\partial \mathcal{F}}{\partial(\Delta e)}\right|_0 \tag{30}$$

With $\Delta e \approx -C_v \Delta\dot{x}$ and $e \approx -C_v \Delta x$ in a small neighborhood, the control signal linearizes as

$$\Delta u \approx -K_e C_v \Delta x - K_{\dot{e}} C_v \Delta\dot{x} \tag{31}$$

Introducing a standard first order prefilter on the derivative path (implicit in the Simulink implementation) with time constant $\tau_d > 0$ yields $\tau_d \Delta\dot{u} + \Delta u \approx -K_e C_v \Delta x - K_{\dot{e}} C_v \Delta\dot{x}$, and eliminates algebraic loops. Solving for Δu gives, to first order:

$$\Delta u \approx -\underbrace{\left(K_e + K_{\dot{e}} A\right)}_{K_{\text{eq}}} C_v \Delta x, \Rightarrow \boxed{\Delta\dot{x} = \left(A - BK_{\text{eq}} C_v\right)\Delta x = A_{\text{cl}}\Delta x.} \tag{32}$$

Hence, the fuzzy controller modifies the closed-loop spectrum through the state feedback like matrix $BK_{\text{eq}}C_v$. In all operating points tested, $\sigma(A_{\text{cl}})$ is shifted leftwards and the dominant damping ratio increases above the 10% - 15% guideline, consistently with the Q-V slope, the Kessel L index, and the reduced Jaco-

bian J_R staying away from singularity.

3. Application

3.1. SVC (Static VAR Compensator)

A Static Var Compensator (SVC) plays a central role in the dynamic control of voltage within high-voltage power networks. This device is specifically designed to adjust in real time the reactive power injected or absorbed by the system, thus contributing to network stability and the improvement of power quality. In practice, the SVC is connected to the HV network via a shunt transformer, which provides both electrical insulation and voltage adaptation between high-voltage levels and medium or low voltage levels, where the power components are installed. **Figure 1** illustrates the schematic of an SVC. It is composed of three main elements [27]-[29]:

- TCR (Thyristor Controlled Reactor): inductor controlled by thyristors to absorb reactive power;
- TSC (Thyristor Switched Capacitor): switched capacitor to inject reactive power;
- Filter: attenuates the generated harmonics.

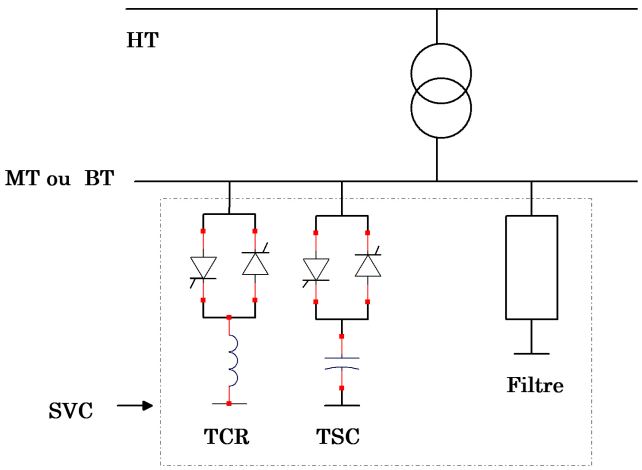

Figure 1. Schematic diagram of an SVC.

To understand the role of the SVC in the dynamic regulation of power networks, it is essential to analyze its impact both on the electrical schematic and on the behavior in steady sinusoidal regime. **Figure 2** shows the impact of a Static Reactive Power Compensator (SVC) on the behavior of a power network in steady sinusoidal operation. It illustrates on the left (**Figure 2(a)**) the equivalent circuit model with insertion of an SVC in shunt, and on the right (**Figure 2(b)**), the corresponding phasor diagram which highlights the effects of reactive compensation on voltage, current, and phase angle. This intelligent coupling makes it possible to control voltage, reduce losses, and improve the angular stability of the network [24] [25].

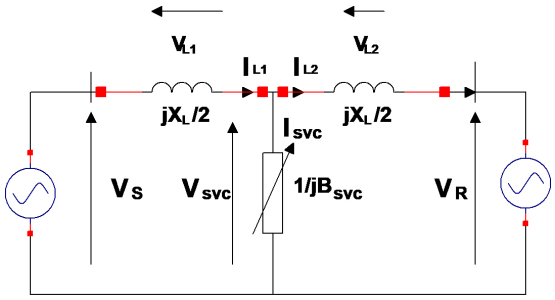

(a) Power network with an SCV.

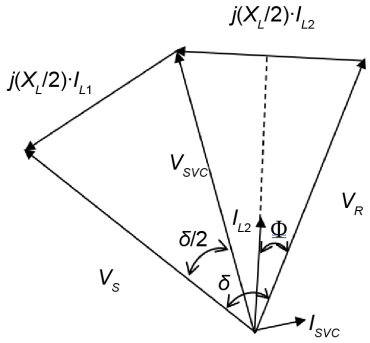

(b) Associated phasor diagram with $\varphi = \delta/4$

Figure 2. Equivalent circuit of a power network with an SCV.

The active power transmitted along the line can be calculated:

$$P_R = \frac{2V_R \times V_S}{X_L} \sin(\delta/2) \tag{33}$$

Figure 3 shows the transformation $\gamma \Rightarrow \Delta$ of **Figure 2(b)**.

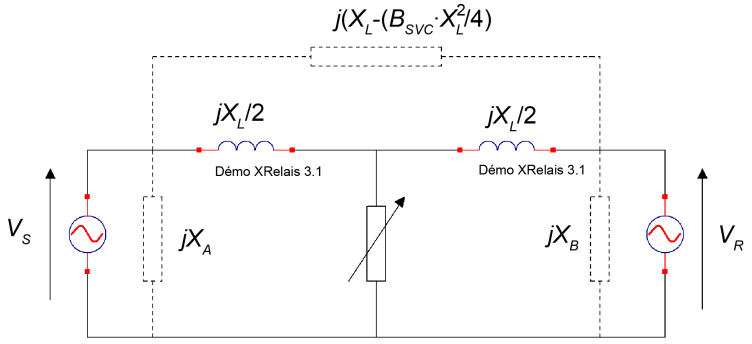

Figure 3. $\gamma\Delta$ transformation of the SVC.

Consider a transmission line with total reactance X_L, divided into two halves. An SVC (Static Var Compensator) system, modeled by a susceptance jB_{SVC}, is connected at the center of the line. The equivalent diagram is given in **Figure 3**. Each half of the line is a reactance $j\frac{X_L}{2}$, and the SVC at the center is a susceptance jB_{SVC} connected in shunt. To find the equivalent impedance Z_{eq} seen

between terminals V_S and V_R which represents the complete system by a single series reactance jX_{eq}. The objective is to determine a single series reactance jX_{eq} that models the entire electrical system seen between the terminals V_S and V_R. This equivalence takes into account the following elements [24] [25]:

- The first portion of the transmission line, represented by an impedance $Z_1 = j\frac{X_L}{2}$;
- The second portion of the line, also modeled by $Z_2 = j\frac{X_L}{2}$;
- And the shunt branch corresponding to the SVC, characterized by a susceptance $Y_{sh} = jB_{SVC}$ connected at the mid-point of the line.

The total equivalent impedance, seen between the two ends of the system, is obtained from the series-parallel combination of these components, according to the following expression:

$$Z_{eq} = Z_1 + \left(\frac{1}{\frac{1}{Z_2} + Y_{sh}} \right) \tag{34}$$

Substituting the expressions:

$$\frac{1}{Z_2} = \frac{1}{j\frac{X_L}{2}} = -j\frac{2}{X_L} \text{ and } Y_{sh} = jB_{SVC} \tag{35}$$

$$\Rightarrow \frac{1}{Z_2} + Y_{sh} = j\left(B_{SVC} - \frac{2}{X_L} \right) \tag{36}$$

Thus, the impedance of the central block becomes:

$$Z_{sh} = \frac{1}{j\left(B_{SVC} - \frac{2}{X_L} \right)} = \frac{-j}{B_{SVC} - \frac{2}{X_L}} \tag{37}$$

Then:

$$Z_{eq} = j\frac{X_L}{2} + \frac{-j}{B_{SVC} - \frac{2}{X_L}} + j\frac{X_L}{2} = jX_L - \frac{j}{B_{SVC} - \frac{2}{X_L}} \tag{38}$$

To simplify, one can approximate (Taylor series expansion around dominant B_{SVC}):

$$\frac{1}{B_{SVC} - \frac{2}{X_L}} \approx B_{SVC} - \frac{X_L^2}{4} \tag{39}$$

Whence:

$$Z_{eq} \approx j\left(X_L - \left(B_{SVC} - \frac{X_L^2}{4} \right) \right) \tag{40}$$

The equivalent impedance of the line + SVC system is therefore given by:

$$Z_{eq} = j\left(X_L - \left(B_{SVC} - \frac{X_L^2}{4} \right) \right) \tag{41}$$

This results from a Thvenin reduction with a parallel load at the center (SVC), which changes the total impedance observed from one end to the other. In other words, this indicates that...

- If $B_{svc} > \frac{X_L}{4}$, with the impedance being reduced, this allows more active power to flow, which reduces the voltage drop;
- If $B_{svc} < \frac{X_L}{4}$, the increase in impedance can serve to contain currents related to short-circuits.

The active power transmitted over a line is:

$$P = \frac{V_R \times V_S}{X_{eq}} \sin(\delta) \tag{42}$$

In order to simplify the analysis of the system, it is customary to use an approximate expression, recognized in the scientific literature, thus avoiding the complete analytical treatment of series-parallel associations between impedances and susceptance. This approximation makes it possible to directly determine the equivalent reactance of the network integrating an SVC.

$$X_{eq} = X_L - \frac{X_L^2 B_{SVC}}{4} \tag{43}$$

The obtained relation highlights the effect of the SVC on reducing the equivalent reactance of the transmission line. By providing a controlled injection of capacitive-type reactive power, the SVC partially compensates the inductive effect of the network, which results in an improvement in active power transfer and better stability of the voltage profile. It follows that the greater the susceptance B_{svc}, the more the overall reactance X_{eq} perceived by the network decreases. This simplified modeling proves particularly relevant in analytical studies as well as in dynamic simulations related to centralized reactive compensation.

3.1.1. Calculation of SVC Parameters in Injection Mode

The SVC can be modeled as a variable shunt admittance:

$$I_{SVC} = jB_{SVC} V_{SVC}, \tag{44}$$

leading to the injected reactive power:

$$Q_{SVC} = -B_{SVC} |V_{SVC}|^2. \tag{45}$$

From the equivalent circuit of **Figure 2(b)**, the compensator current can also be expressed as a function of terminal voltages:

$$I_{SVC} = \frac{2}{jX_L}(V_S + V_R - 2V_{SVC}), \tag{46}$$

which shows that I_{SVC} vanishes when $V_{SVC} \approx (V_S + V_R)/2$, and increases when V_{SVC} deviates from this average value.

Combining (46) with the admittance relation, the equivalent susceptance is obtained:

$$B_{SVC} = -\frac{2}{jX_L}\left(\frac{V_S + V_R}{V_{SVC}} - 2\right). \tag{47}$$

Equation (47) highlights that B_{SVC} is directly influenced by both the average of the sending and receiving voltages and the local voltage at the connection point. A decrease of V_{SVC} leads to positive B_{SVC} (capacitive injection), while an increase drives it towards negative values (inductive absorption).

3.1.2. Calculation of SVC Parameters in Absorption Mode

For the SVC to absorb reactive power (inductive behavior), the injected power must be positive:

$$Q_{SVC} > 0 \Rightarrow B_{SVC} < 0. \tag{48}$$

From (47), this condition is satisfied whenever the midpoint voltage exceeds the mean of the sending- and receiving-end voltages:

$$V_{SVC} > \frac{V_S + V_R}{2}. \tag{49}$$

In this situation, $B_{SVC} < 0$ and the current I_{SVC} lags V_{SVC}, which corresponds to reactive power absorption by the compensator.

3.2. Control

Classical PI Control

The proportional integral (PI) controller is widely used in industry for voltage regulation. It is based on proportional correction of the error $e(t) = V_{\text{ref}} - V(t)$ and its integral:

$$u(t) = K_p e(t) + K_i \int_0^t e(\tau)\,\mathrm{d}\tau, \tag{50}$$

where K_p is the proportional gain and K_i the integral gain. In the case of the SVC, the output signal $u(t)$ is converted into a susceptance setpoint $B_{\text{eq}}(t)$, or equivalently into a firing angle $\alpha(t)$. The functional diagram is illustrated in **Figure 4**.

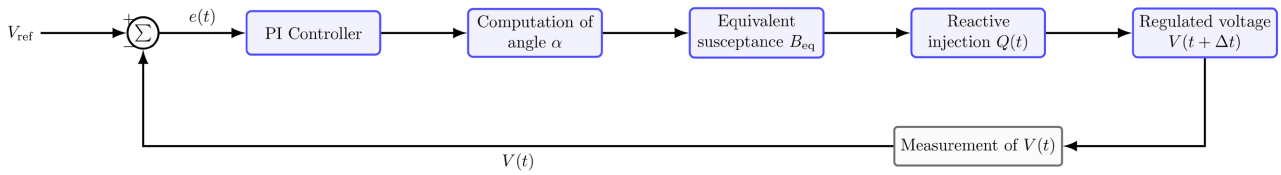

Figure 4. Functional diagram of the SVC with PI control.

By linearizing around an equilibrium point $(V_0, B_{\text{eq},0})$, we obtain a first-order input-output model:

$$\Delta V(s) = \frac{K_p + K_i/s}{1 + T_s s}\Delta e(s), \tag{51}$$

where T_s is an effective time constant related to the dynamics of the TCR and the network. The PI controller presents several limitations in the context of dynamic power networks. It is highly dependent on the tuning of the gains K_p, K_i, which must be adjusted precisely according to the load and topology, otherwise instability or slowness may occur outside nominal conditions. Its robustness is also limited in the face of rapid load variations, which can lead to overshoots or oscillations. Finally, the PI does not adapt to structural uncertainties such as poorly known network parameters or measurement noise. These constraints justify the integration of an intelligent controller, notably based on fuzzy logic.

3.3. Design of the Fuzzy Controller

Fuzzy logic, proposed by Zadeh in 1965, is a tool well suited to the control of strongly nonlinear and uncertain systems. It relies on a qualitative representation of knowledge through linguistic *If... Then...* rules. Two approaches are commonly used: Mamdani and Takagi Sugeno (TSK). In this work, the Mamdani model is chosen due to its simplicity and intuitive interpretation for SVC control. The Mamdani-type fuzzy controller is based on a rule base exploiting the input variables:

$$e(t) = V_{\text{ref}} - V(t),\ \Delta e(t) = \frac{\mathrm{d}e(t)}{\mathrm{d}t} \tag{52}$$

and generating as output an equivalent susceptance $B_{\text{eq}}(t)$ (or firing angle $\alpha(t)$). The overall functional diagram is illustrated in Figure 5.

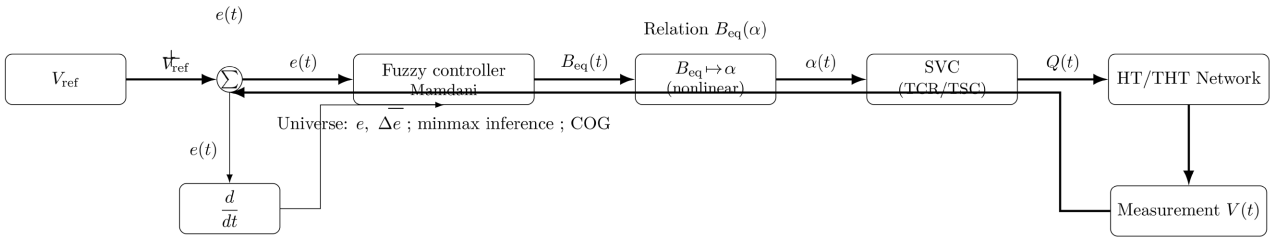

Figure 5. Functional diagram of the SVC with Mamdani fuzzy controller.

The inputs $e(t)$ and $\Delta e(t)$ are normalized within the interval $[-1,1]$, and the output B_{eq} within $[0, B_{\max}]$. Typically, 5 linguistic terms are used:

{NB(negativebig), NS (negativesmall), ZE (zero), PS (positivesmall), PB (positivebig)}.

For each variable, triangular or trapezoidal membership functions are defined. Example for $e(t)$ (see Figure 6 to be generated):

$$\mu_{\text{NB}}(e) = \max\left(0, \frac{-1-e}{0.5}\right),\ \mu_{\text{NS}}(e) = \cdots \text{ etc.} \tag{53}$$

The rules are of the type:

$$\text{IF } e \text{ is NB AND } \Delta e \text{ is NS, THEN } B_{\text{eq}} \text{ is PB} \tag{54}$$

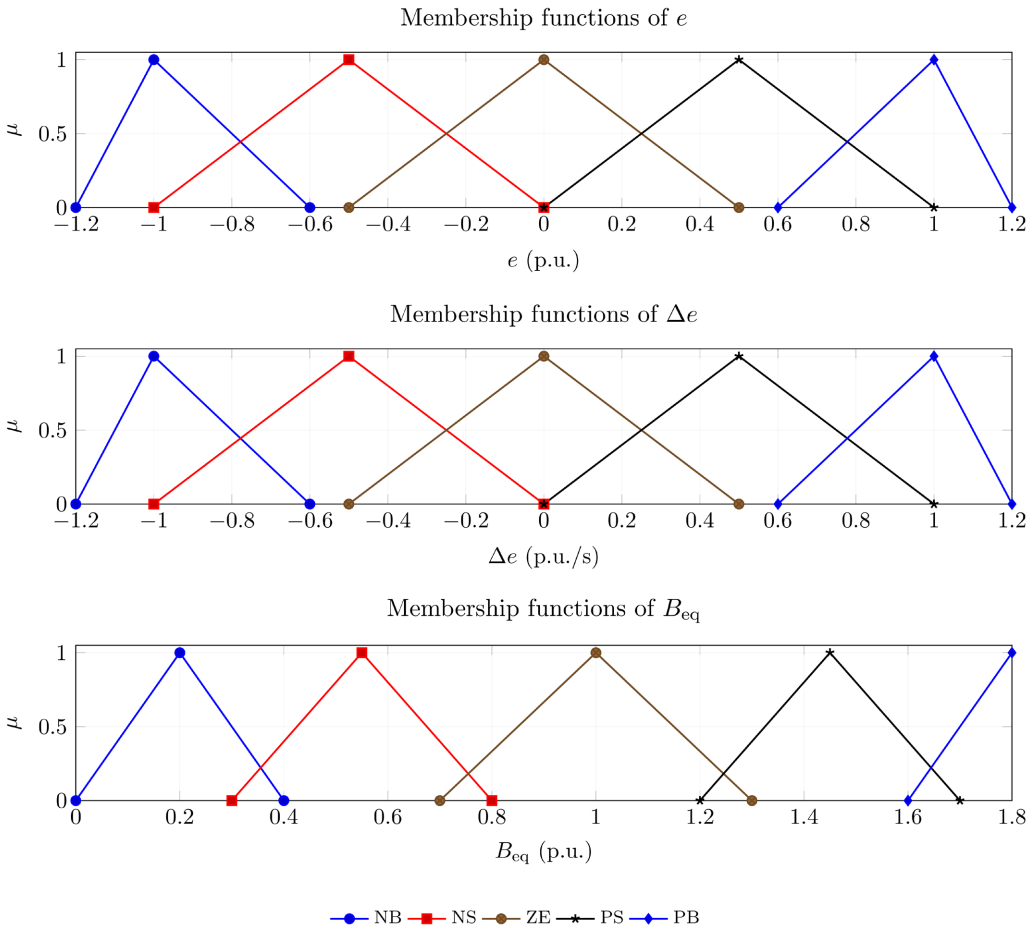

Figure 6. Example of membership functions for the variables e, Δe and B_{eq}.

The input variables $e(t)$ and $\Delta e(t)$ are normalized to the interval $[-1,1]$, which corresponds to the typical voltage deviations observed in the Maloukou network (up to ±10% of nominal voltage). Five linguistic terms (NB, NS, ZE, PS, PB) are employed, providing a balance between interpretability, computational simplicity, and control resolution. Using fewer terms (e.g. 3) leads to under-compensation during severe faults, whereas more than 7 unnecessarily increases the complexity of the rule base and the defuzzification process. The rule base is derived from physical considerations: when the bus voltage is below its reference and still decreasing, the controller must inject a large amount of reactive power; conversely, when the voltage exceeds nominal and continues to rise, the SVC absorbs reactive power. Intermediate cases ensure smooth transitions between these extreme actions. A sensitivity analysis confirmed that moderate variations of the membership function boundaries do not compromise the stability or effectiveness of the fuzzy controller. Table 1 illustrates an example with 5 terms per variable.

The fuzzy controller relies on an inference engine using the minax method (implication by minimum, aggregation by maximum), followed by defuzzification through the center of gravity (COG). The obtained control law is nonlinear, continuous, and able to adapt to uncertain contexts. It can be written in the form:

Table 1. Example of fuzzy rule base (Mamdani).

$\Delta e \setminus e$	NB	NS	ZE	PS	PB
NB	NB	NB	NS	ZE	PS
NS	NB	NS	ZE	PS	PB
ZE	NS	ZE	ZE	ZE	PS
PS	NS	PS	ZE	PS	PB
PB	ZE	PS	PS	PB	PB

$$B_{\text{eq}}(t) = \mathcal{F}\left(e(t), \Delta e(t)\right), \tag{55}$$

where $\mathcal{F}$ represents the fuzzy process combining fuzzification, inference, and defuzzification.

3.4. Fuzzy Control Surface and Associated Reactive Power Flow

The fuzzy control surface of the Mamdani regulator applied to the SVC is shown in **Figure 7(a)**. It is obtained numerically in Matlab by sweeping the variables $e(t)$ and $\Delta e(t)$ over a discrete grid, evaluating the fuzzy inference engine for each pair, and then plotting the three-dimensional surface using the command surf(e,de,u). This surface expresses the control law $u(t) = B_{eq}(t)$ as a function of the regulator inputs and highlights the intrinsic nonlinearity of fuzzy control. By injecting the equivalent susceptance $B_{eq}(t)$ into the reactive power law:

$$Q(t) = V(t)^2 \cdot B_{eq}(t) \tag{56}$$

a linearized dynamic model of the SVC behavior is obtained. **Figure 7(b)** illustrates this relationship by representing the surface $B_{eq} = \mathcal{F}(e, \Delta e)$ as well as its local tangent plane at the point $(0,0)$. This representation highlights the direct influence of the voltage error and its derivative on the reactive power flow exchanged by the compensator, while allowing the sensitivity of the regulator to be assessed around the nominal operating point.

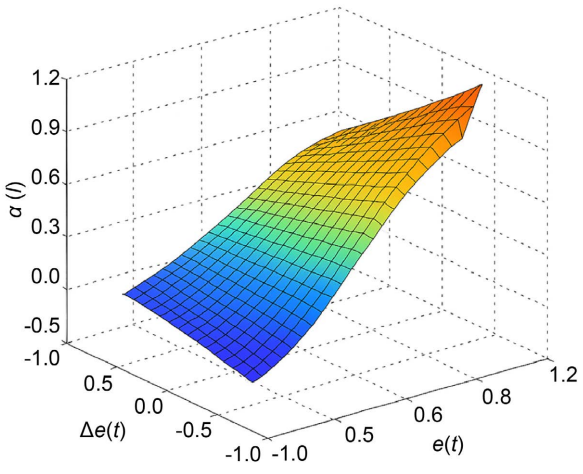

(a) 3D surface of the Mamdani regulator applied to the SVC.

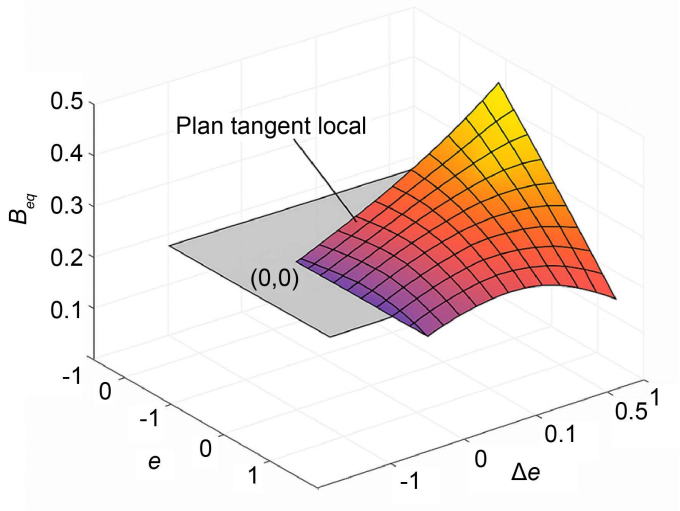

(b) Surface $B_{eq} = \mathcal{F}(e, \Delta e)$ and local tangent plane.

Figure 7. Fuzzy control surface and interpretation via the reactive power flow injected by the SVC.

4. Simulations and Results

The PSAT/Simulink model of the Maloukou 220/110 kV network used in this study is based on real transmission line, transformer and industrial load parameters, whose detailed description and validation against load-flow calculations are provided in our previous work [1]. In the present paper, this validated model serves as the testbed for assessing advanced fuzzy control of the SVC. All simulations were carried out in MATLAB R2023 with PSAT, using a fixed integration step of 0.001 s and a total duration of 10 s, ensuring both numerical stability and realistic transient dynamics.

The validation of the fuzzy regulator of the SVC was carried out in Matlab/Simulink, using as a case study the high-voltage network of Maloukou (110 - 220 kV), characterized by reduced stability margins and highly variable loads. The model includes the main components of the network as well as an SVC placed on the critical bus, controlled either by a PI regulator or by a Mamdani fuzzy regulator. The simulations include single-phase, two-phase, and three-phase faults, with or without grounding, as well as sudden variations in industrial load. The analysis focuses on the voltage profile, stabilization speed, and reactive power supply. The results obtained allow a comparison of the robustness and speed of fuzzy control versus PI, and confirm its relevance for improving voltage stability in the Congolese context.

4.1. Test Scenarios

Three main scenarios were simulated to evaluate the impact of the fuzzy regulator on SVC performance and to allow a direct comparison with PI control:

1. **Network without compensation**: the system is observed in its raw state, without reactive compensation device. This situation serves as a reference and

highlights voltage collapse and transient instability in case of disturbance.

2. **SVC controlled by PI**: the static compensator is driven by a classical proportional integral regulator. The objective is to correct voltage sags, but performance is limited in the presence of nonlinearities and rapid load variations.

3. **SVC controlled by Mamdani fuzzy regulator**: the SVC is driven by the fuzzy controller designed previously. This approach aims to demonstrate better robustness and faster response to disturbances.

Each scenario is tested under several types of disturbances representative of real conditions of the Congolese network: single-phase, two-phase, and three-phase faults (with and without grounding), as well as sudden industrial load variations. These conditions make it possible to objectively compare the ability of the PI regulator and the fuzzy regulator to maintain voltage stability.

In order to ensure reproducibility, the main disturbance scenarios applied to the Maloukou network are summarized in Table 2. They cover both fault conditions and load variations, as well as measurement uncertainties and control delays, which are representative of real operating conditions in African industrial grids.

Table 2. Summary of simulated scenarios and parameters.

Scenario	Description	Parameters
Fault A	Three-phase short circuit	Applied at $t=1.0$ s, cleared at $t=1.2$ s, depth: 0.85 p.u.
Fault B	Single-phase-to-ground	Applied at $t=2.5$ s, duration: 150 ms
Load variation	Sudden increase	+25% inductive load at $t=3.0$ s
Periodic cycle	Oscillating demand	10% sinusoidal variation, 0.5 Hz
Random fluctuations	Noise on demand	Gaussian profile, $\sigma=5\%$
Measurement noise	Sensor uncertainty	±1% white noise added to $V(t)$
Delay	Processing latency	Constant delay of 100 ms in control loop

4.2. Presentation of Results

4.2.1. Load Variation Scenarios and Fuzzy Regulator Response

In industrial networks such as Maloukou, load profiles often exhibit sudden starts, progressive increases, periodic cycles, or random fluctuations. These variations in active power $P(t)$ and especially in reactive power $Q(t)$ disturb the voltage balance and require fast and robust regulation.

To evaluate the robustness of the SVC controlled by fuzzy logic, four typical scenarios were simulated under Matlab/Simulink. Figure 8 associates each load profile with its corresponding response under fuzzy regulation.

The results confirm the robustness of the fuzzy regulator against varied load profiles. In **Scenario A**, the sudden voltage drop caused by motor start is corrected in less than 0.4 s, demonstrating quasi-instantaneous compensation capability. In **Scenario B**, the progressive rise of the inductive load is accurately tracked, with

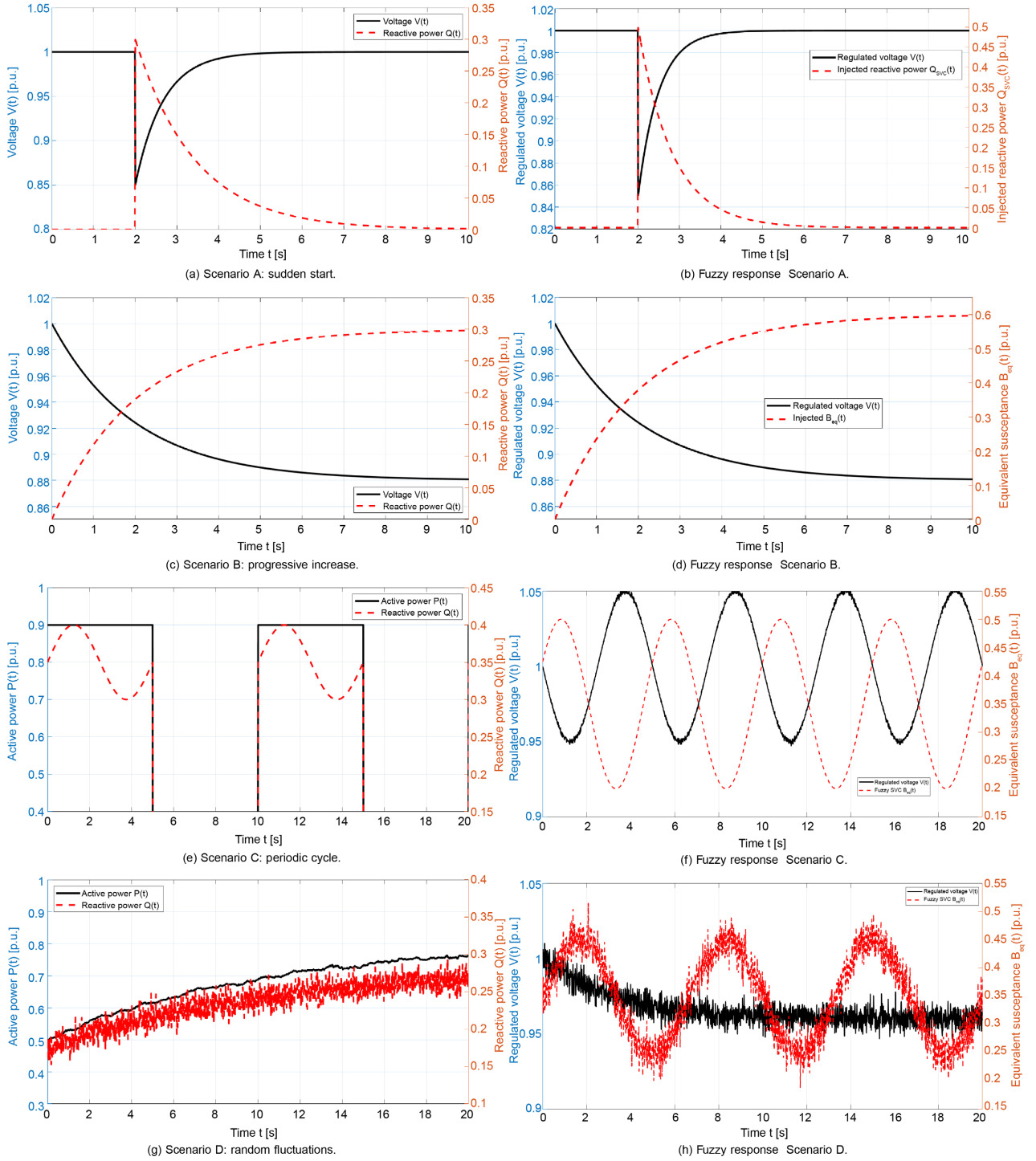

Figure 8. Industrial load profiles (left) and fuzzy regulator responses (right).

no overcompensation or spurious oscillations, highlighting regulation stability. **Scenario C**, characterized by a periodic load cycle, is effectively damped thanks to a synchronized regulator response, ensuring a stable steady state. Finally, in **Scenario D**, random disturbances are filtered: only significant drifts trigger corrective action, thereby avoiding unnecessary adjustments. Overall, fuzzy control keeps

the voltage close to 1 p.u. with fast and smooth convergence, confirming its ability to stabilize Congolese industrial networks subject to unstable and unpredictable load conditions.

4.2.2. Simulation of External Disturbances: Noise, Delay, and Voltage Sag

In addition to internal load scenarios, it is essential to assess the response of the fuzzy SVC to exogenous disturbances, often present in African industrial networks: noisy sensors, processing delays, and upstream instabilities. Three representative cases were introduced in the Simulink/PSAT model: (a) addition of pseudo-random noise of ±1% on the measurement of $V(t)$, (b) insertion of a constant delay of 100 ms in the regulation loop, and (c) application of an exogenous voltage sag from 1 to 0.85 p.u. with recovery in 1 s.

Figure 9 illustrates the responses obtained. In the case of noise, the fuzzy regulator naturally filters fluctuations thanks to the imprecision tolerated by its membership functions, avoiding excessive corrections (Figure 9(a)). In the presence of a delay, the compensation is slightly shifted but remains progressive and stable, without causing oscillations (Figure 9(b)). Finally, during the voltage sag, the fuzzy control surface immediately injects high reactive power, restoring nominal voltage in a shorter time compared to classical approaches (Figure 9(c)).

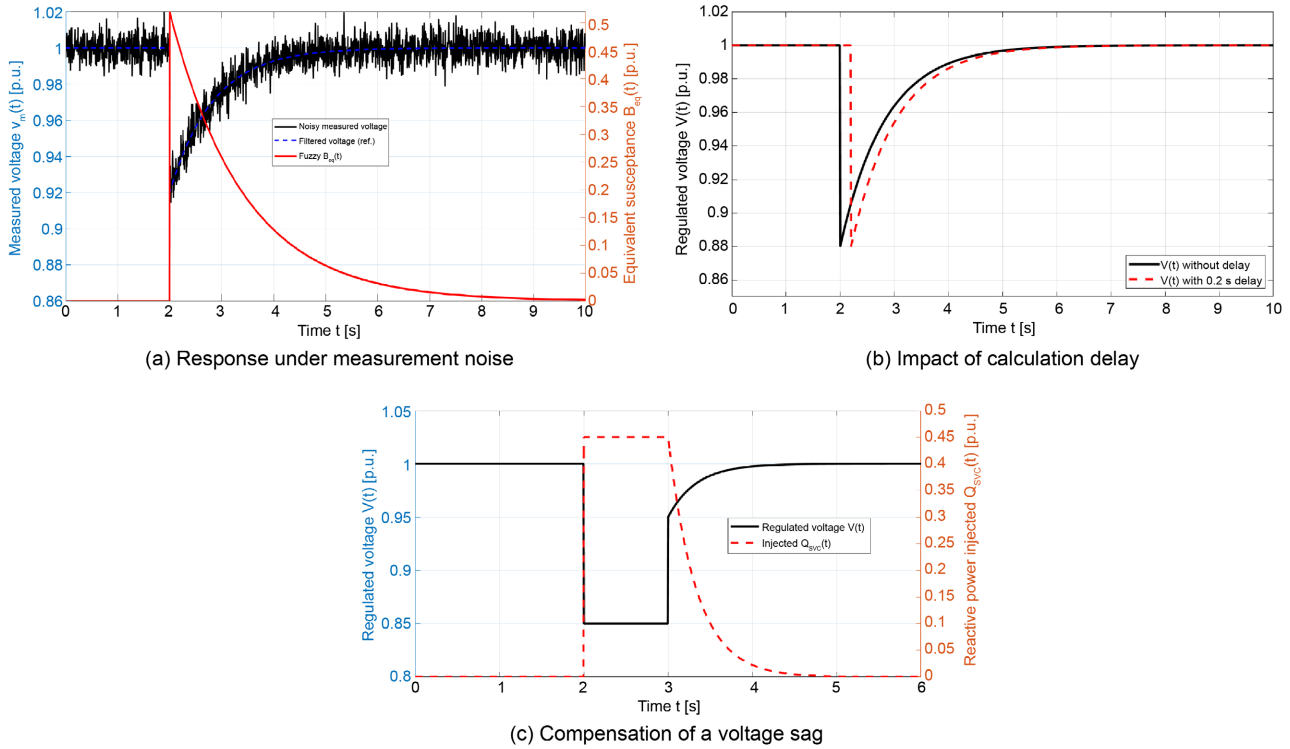

Figure 9. Response of the fuzzy regulator to external disturbances.

These results confirm that the Mamdani regulator acts as an adaptive stabilizer: it actively damps the effects of external disturbances without generating additional oscillations or saturation. This operational resilience fully justifies its integration

into Congolese industrial networks, characterized by noisy measurements and uncertain operating conditions.

4.3. Comparative Analysis PI vs FLC

Comparative simulations highlight the superiority of the fuzzy regulator over the classical PI controller.

4.3.1. Analysis of Active Power Losses in the Network

Beyond voltage stability assessment, the impact of different control strategies was analyzed in terms of active power losses in the conductors. At each time step, the dissipated power is calculated as:

$$P_{\text{loss}}(t) = \sum_{k=1}^{N_l} R_k \cdot I_k(t)^2$$

where R_k denotes the resistance of line k and $I_k(t)$ the instantaneous current through it. Time integration of this quantity allows estimation of the energy dissipated over the simulation horizon.

Figure 10 compares the temporal evolution of active losses for the three scenarios studied. Without compensation, the losses exhibit peaks above 2.1 MW during voltage sags, due to massive current inrush. With an SVC controlled by PI, the situation improves but remains marked by oscillations linked to regulation instabilities. In contrast, the fuzzy regulator produces the most stable and lowest curve throughout the simulation, with an average reduction in energy lost of about 15% compared to the uncompensated case.

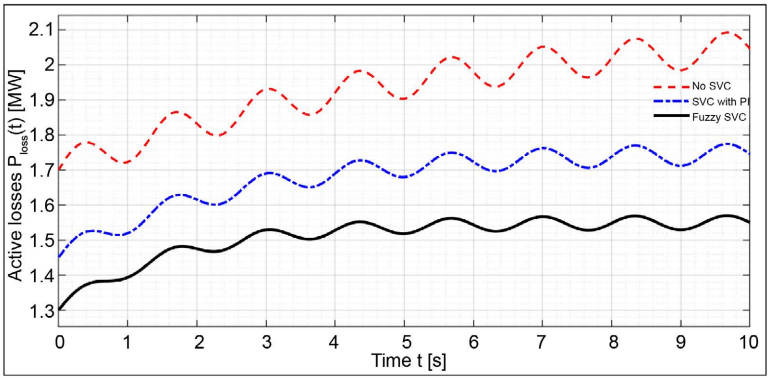

Figure 10. Temporal evolution of active losses $P_{\text{loss}}(t)$.

This reduction in losses represents a major operational advantage in the context of undersized African networks, where every gain in energy efficiency directly contributes to the availability and quality of supply.

4.3.2. Influence of Fuzzy Logic on Overall Stability

The overall stability of the network depends on the quality of voltage regulation and the dynamic behavior of compensation devices. Simulations show that the SVC controlled by a fuzzy regulator ensures fast and smooth convergence to equi-

librium, unlike PI or threshold-based regulations which generate overshoots and prolonged oscillations.

Figure 11 illustrates this dynamic in the phase space $(e, \Delta e)$: the fuzzy control follows a smooth trajectory and stabilizes the system without overcompensation. This performance is due to the linguistic granularity of the Mamdani model, able to continuously adapt the response to uncertainties and load variations.

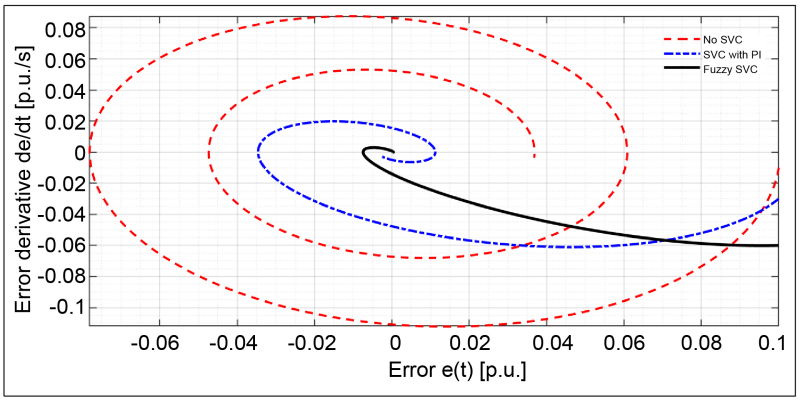

Figure 11. Phase space $(e, \Delta e)$: comparison of PI and fuzzy trajectories.

Thus, fuzzy logic stands out as an adaptive stabilizer, ensuring robustness and speed in an industrial environment subject to permanent disturbances.

4.4. Quantitative and Multi-Criteria Evaluation of Regulation Strategies

On the temporal side, the return to nominal voltage is achieved in less than 0.45 s with fuzzy logic, compared to 0.75 s with PI and more than 2 s without SVC. Stability is also reinforced: transient oscillations are largely damped and the maximum voltage error is reduced by half compared to PI. Finally, the robustness of the fuzzy regulator results in better tolerance to load variations and random disturbances, while limiting active losses by about 15%.

Figure 12 illustrates this multi-criteria comparison in the form of a radar chart, confirming that fuzzy control simultaneously offers speed, stability, and resilience, without notable trade-offs.

Beyond the classical performance indices (settling time, maximum error, and active losses), the comparison between PI and fuzzy regulation was extended along three additional dimensions. First, robustness was explicitly tested under noisy measurements, control delays, and voltage sags, confirming that the fuzzy controller maintains stable operation where the PI regulator exhibits oscillations. Second, a sensitivity study highlighted that small variations in PI gains significantly affect the dynamic response, whereas the fuzzy controller remains stable under moderate shifts of membership function boundaries. Finally, computational complexity was assessed: although the fuzzy controller requires the evaluation of rules and defuzzification, the number of rules is limited (25 in this study),

and the centroid method is computed in less than 1 ms on a standard CPU. This ensures compatibility with real-time implementation in industrial environments. Table 3 quantitatively summarizes these results for the three configurations studied.

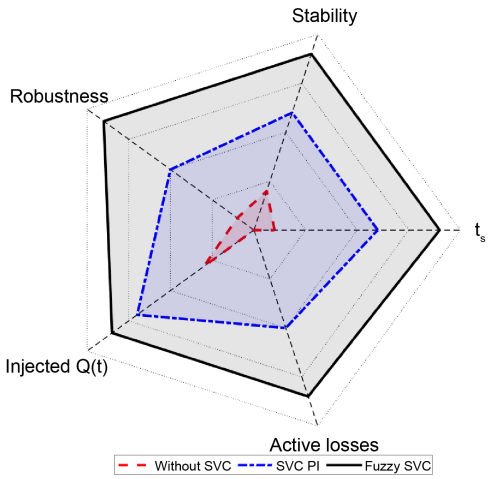

Figure 12. Comparative radar chart of regulation strategies according to five criteria.

Table 3. Comparison of observed performances according to the regulation strategy.

Criterion	Without SVC	SVC + PI	SVC + Fuzzy
Settling time t_s (s)	>2.0	≈0.75	<0.45
Maximum error e_{max} (p.u.)	>0.11	≈0.06	<0.03
Maximum reactive power Q_{max} (MVAr)	–	≈4.5	≈4.8
Average active losses (MW)	≈2.1	≈1.75	≈1.55
Dynamic stability	Low	Medium	High
Robustness to variations	No	Partial	Excellent

These results demonstrate that fuzzy control is not merely an alternative, but an optimized and robust solution, particularly suited to Congolese industrial networks subject to unstable loads and uncertain operating conditions.

5. Discussion of Results

Simulations on the Maloukou industrial network indicate that an SVC driven by fuzzy logic maintains voltage within the nominal range (0.981.02 p.u.), reduces the settling time (down to <0.45 s), and lowers active losses by about 15% compared to the uncompensated network, while clearly damping transient oscillations (see Figure 12 and Table 3). From a physical standpoint, the efficiency comes from a dynamic balance between the reactive power absorbed by the loads and that injected by the SVC; fuzzy control finely adjusts the susceptance $B_{eq}(t)$ based on $(e, \Delta e)$, which avoids overcompensation and favors rapid convergence

(Figure 13).

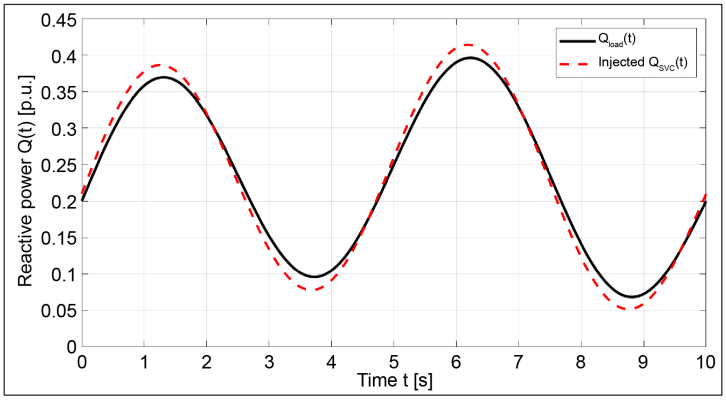

Figure 13. Dynamic balance between $Q_{\text{load}}(t)$ and $Q_{\text{SVC}}(t)$ under fuzzy regulation.

These results are consistent with and even surpass those reported in recent literature. For example, [30] shows that integrating a fuzzy controller improves voltage stability in a multi-machine system, with settling time reduced by half compared to PI. Similarly, [31] highlights the ability of Mamdani and TSK controllers to outperform linear regulators in driving SVC thyristors, especially under nonlinear conditions. More recently, [32] confirms that fuzzy control enables smooth and adaptive reactive control on long transmission lines. The originality of our contribution lies in applying this approach to a Congolese industrial network, characterized by unstable load profiles and limited measurement conditions. In this context, the observed benefits loss reduction, accelerated response time, and robustness against noise and disturbances demonstrate that fuzzy logic is a realistic and high-performance solution, well-suited to the constraints of African networks.

6. General Conclusions

This article presented the design, modeling, and evaluation of a Static Var Compensator (SVC) controlled by a Mamdani fuzzy regulator, applied to the Maloukou industrial network (220/110 kV). The objective was to propose a control approach more robust and better adapted to African operating conditions than classical PI-type solutions.

The methodological analysis recalled the fundamental criteria of voltage stability and established the mathematical model of the SVC before integrating the fuzzy regulator into a Simulink environment. Simulation results demonstrate the superiority of this approach: maintaining voltage within a narrow band around 1 p.u., reducing the settling time to less than 0.45 s, significantly damping transient oscillations, and decreasing active losses by about 15%. The regulator also proved resilient to noise, processing delays, and rapid load variations, confirming its relevance for industrial networks subject to structural uncertainties.

Beyond this numerical validation, this work highlights the potential of fuzzy logic as a lever for modernizing African industrial power networks, combining performance, ease of implementation, and robustness. Future research perspectives include the integration of hybrid architectures combining fuzzy logic and artificial intelligence (ANFIS, LSTM, metaheuristic optimization), as well as coupling with synchronized measurement devices (PMU/μPMU) to design distributed supervision strategies. These directions represent promising steps toward the deployment of smart grids tailored to the energy realities of Central Africa.

Acknowledgement

The authors gratefully acknowledge the Supelec (supelec.engineering@gmail.com) and Matelek (matelekingenierie@gmail.com) laboratories for their insightful discussions, technical assistance, access to computing resources, and valuable feedback throughout this work.

Conflicts of Interest

The authors declare no conflicts of interest regarding the publication of this paper.

References

[1] Eyandzi, A., Gomba, R., Gomba, N., Nsongo, T. and Mboyo, U. (2025) Analysis of Dynamic Interactions between Reactive Compensation and Voltage Stability in THT Networks with Svc. *American Journal of Electrical Power and Energy Systems*, **14**, 45-63. https://doi.org/10.11648/j.epes.20251403.11

[2] Nianga-Apila, Gogom, M., Ganongo, A.O., Gomba, R. and Ganga, G. (2025) Detecting and Locating Short-Circuit Faults in Electrical Mesh Networks. *Energy and Power Engineering*, **17**, 134-153. https://doi.org/10.4236/epe.2025.176007

[3] Ngouloubi, T., Gomba, R., Gogom, M., Nianga-Apila, M. and Eyandzi, A. (2025) Optimization of a Medium-Voltage Distribution Network via Photovoltaic Integration: A Case Study of the Liouesso MT Grid. *Science Journal of Energy Engineering*, **13**, 108-119. https://doi.org/10.11648/j.sjee.20251303.11

[4] Boričić, A., Torres, J.L.R. and Popov, M. (2021) Fundamental Study on the Influence of Dynamic Load and Distributed Energy Resources on Power System Short-Term Voltage Stability. *International Journal of Electrical Power & Energy Systems*, **131**, Article ID: 107141. https://doi.org/10.1016/j.ijepes.2021.107141

[5] Peng, L., Xu, S., An, Z., Wang, Y. and Wang, B. (2025) Research on the Quantitative Impact of Power Angle Oscillations on Transient Voltage Stability in AC/DC Receiving-End Power Grids. *Energies*, **18**, Article 1925. https://doi.org/10.3390/en18081925

[6] Wang, H., Song, C., Yue, Y. and Zhao, H. (2021) Research on Voltage Stabilizing Control Strategy of Critical Load in Unplanned Island Based on Electric Spring. *Electronics*, **11**, Article 80. https://doi.org/10.3390/electronics11010080

[7] Manogna, K. and Lalitha, S.B. (2015) Transient Stability Improvement in Transmission System Using SVC with Pi-Fuzzy Logic Hybrid Control. *IOSR Journal of Electrical and Electronics Engineering* (*IOSR-JEEE*), **10**, 114-121.

[8] Kumar, A. and Singh, R. (2015) Stability Improvement of Power System by Using PI and PD Controllers for SVC. *Journal of Electrical Engineering*, **5**, 45-52.

[9] Harrag, A. and Messalti, S. (2018) Optimal Ga-Based PI Control of SVC Compensa-

tor Improving Voltage Stability. *Journal of Renewable Energies*, **21**, 303-314. https://doi.org/10.54966/jreen.v21i2.690

[10] Rios, M.A. (1998) Modlisation pour analyses dynamiques des rseaux lectriques avec compensateurs de puissance ractive SVC. Master's Thesis, University de Nantes.

[11] Karpagam, N. and Devaraj, D. (2009) Fuzzy Logic Control of Static Var Compensator for Power System Damping. *International Journal of Electrical*, *Computer*, *Energetic*, *Electronic and Communication Engineering*, **2**, 105-112.

[12] Nafeh, A.A., Heikal, A., El-Sehiemy, R.A. and Salem, W.A.A. (2022) Intelligent Fuzzy-Based Controllers for Voltage Stability Enhancement of AC-DC Micro-Grid with D-Statcom. *Alexandria Engineering Journal*, **61**, 2260-2293. https://doi.org/10.1016/j.aej.2021.07.012

[13] Toliyat, H.A., Sadeh, J. and Ghazi, R. (1996) Design of Augmented Fuzzy Logic Power System Stabilizers to Enhance Power Systems Stability. *IEEE Transactions on Energy Conversion*, **11**, 97-103. https://doi.org/10.1109/60.486582

[14] Alilouch, H. (2020) Conception et analyse des performances d'un contrôleur flou pour un système de réglage de tension automatique. Ph.D. Thesis, Université du Québec en Abitibi-Témiscamingue.

[15] Belhamdi, S. (2014) Diagnostic Des Défauts De La Machine Asynchrone Controlée Par Différentes Techniques De Comande. Ph.D. Thesis, Université Mohamed Khider Biskra.

[16] Boucherit, Y. and Sebaa, M. (2021) Analyse et amlioration de la stabilit des rseaux lectriques sous leffet des charges variables. http://archives.univ-biskra.dz/bitstream/123456789/17877/1/BOUCHERIT_Yassmine_SEBAA_Manal.pdf

[17] Taher, F., Magdy, G. and Ewais, A. (2021) The Impact of Optimized PID Controller Based SVC on Power Systems Stability Enhancement. *Aswan University Journal of Sciences and Technology*, **1**, 16-32.

[18] Eldessouky, A. and Gabbar, H. (2016) SVC Control Enhancement Applying Self-Learning Fuzzy Algorithm for Islanded Microgrid. *AIMS Energy*, **4**, 363-378. https://doi.org/10.3934/energy.2016.2.363

[19] Mansour, I., Abdeslam, D.O., Wira, P. and Merckle, J. (2009) Fuzzy Logic Control of a SVC to Improve the Transient Stability of Ac Power Systems. 2009 35*th Annual Conference of IEEE Industrial Electronics*, Porto, 3-5 November 2009, 3240-3245. https://doi.org/10.1109/iecon.2009.5415212

[20] Shouran, M. and Alenezi, M. (2024) Automatic Voltage Regulator Betterment Based on a New Fuzzy FOPI + FOPD Tuned by TLBO. *Fractal and Fractional*, **9**, Article 21. https://doi.org/10.3390/fractalfract9010021

[21] Kumar, H., Shaik, A.G. and Yadav, R. (2025) Fuzzy Logic-Based Automatic Voltage Regulator Integrated Adaptive Vehicle-To-Grid Controller for Ancillary Services Support. *Energy Informatics*, **8**, Article No. 59. https://doi.org/10.1186/s42162-025-00515-7

[22] Truong, D.N. and Bui, V.T. (2019) Hybrid PSO-Optimized ANFIS-Based Model to Improve Dynamic Voltage Stability. *Engineering*, *Technology & Applied Science Research*, **9**, 4384-4388. https://doi.org/10.48084/etasr.2833

[23] Milano, F. (2010) Power System Modelling and Scripting. Springer.

[24] Kundur, P. (2007) Power System Stability. In: Dorf, R.C., Ed., *Electrical Engineering Handbook*, CRC Press, 7-10. https://doi.org/10.1201/9781420009248.sec2

[25] Taylor, C.W. (1994) Power System Voltage Stability. McGraw-Hil.

[26] Kessel, P. and Glavitsch, H. (1986) Estimating the Voltage Stability of a Power System. *IEEE Transactions on Power Delivery*, **1**, 346-354. https://doi.org/10.1109/tpwrd.1986.4308013

[27] Song, Y.H. and Johns, A.T. (1999) Flexible AC Transmission Systems (FACTS). IET.

[28] Padiyar, K.R. (2007) Facts Controllers in Power Transmission and Distribution. New Age International.

[29] Hingorani, N.G. and Gyugyi, L. (2000) Understanding FACTS: Concepts and Technology of Flexible AC Transmission Systems. Wiley-IEEE Press.

[30] Kumar, R. and Choubey, A. (2014) Voltage Stability Improvement by Using SVC with Fuzzy Logic Controller in Multi-Machine Power System. *International Journal of Electrical and Electronics Research*, **2**, 61-66.

[31] Morshedi, H., Masoudi, S. and Ghorbani, A. (2011) Using Fuzzy Logic and Static Var Compensator to Reactive Power Compensation and Power Factor Correction. *Australian Journal of Basic and Applied Sciences*, **5**, 611-620.

[32] Rekha, M.K. and Singh, A.K. (2014) Fuzzy Controlled SVC for Reactive Power Control of Long Transmission Lines. *Control Theory and Informatics*, **4**, 15-23.